

Finite-size scaling and latent heat at the gonihedric first-order phase transition

Wolfhard Janke¹, Marco Mueller¹ and Desmond A. Johnston²

¹ Institut für Theoretische Physik, Universität Leipzig, Postfach 100 920, 04009 Leipzig, Germany

² Department of Mathematics, School of Mathematical and Computer Sciences, Heriot-Watt University, Riccarton, Edinburgh EH14 4AS, Scotland

E-mail: Wolfhard.Janke@itp.uni-leipzig.de

Abstract. A well-known feature of first-order phase transitions is that fixed boundary conditions can strongly influence finite-size corrections, modifying the leading corrections for an L^3 lattice in $3d$ from order $1/L^3$ under periodic boundary conditions to $1/L$. A rather similar effect, albeit of completely different origin, occurs when the system possesses an exponential low-temperature phase degeneracy of the form 2^{3L} which causes for periodic boundary conditions a leading correction of order $1/L^2$ in $3d$. We discuss a $3d$ plaquette Hamiltonian (“gonihedric”) Ising model, which displays such a degeneracy and manifests the modified scaling behaviour. We also investigate an apparent discrepancy between the fixed and periodic boundary condition latent heats for the model when extrapolating to the thermodynamic limit.

Generic features of first-order phase transitions in numerical studies are rarely discussed compared to the universal aspects of second-order phase transitions [1]. Numerical investigations always rely on observations of finite systems, but often one is really interested in the properties of macroscopic systems. The thermodynamic limit is approached by finite-size scaling, a theory that was developed in the 1980’s [2, 3, 4] and refined [5, 6, 7, 8, 9]. Employing a simple heuristic two-phase model [10] rather than the full-blown Pirogov-Sinai theory [11], corrections to typical quantities due to finiteness of the lattice can be calculated already to some extent. For a *periodic* $3d$ system residing on a cube with volume $V = L^3$, the maximum of the specific heat $C_V(\beta, L) = -\beta^2 \partial e(\beta, L) / \partial \beta$ with $e(\beta, L) = \langle E \rangle(\beta, L) / L^3$ denoting the energy per site is according to the two-phase model [10] given by

$$C_V^{\max}(L) = L^3(\beta^\infty \Delta \hat{e} / 2)^2. \quad (1)$$

Here, β^∞ is the inverse transition temperature of a system with infinitely many sites and $\Delta \hat{e} = \hat{e}_d - \hat{e}_o$ is its latent heat, the difference between the energy of the disordered and ordered phases. The position of the maximum is calculated using an expansion around β^∞ [10, 12] and found to be located at inverse temperature

$$\beta^{C_V^{\max}}(L) = \beta^\infty - \frac{\ln q}{L^3 \Delta \hat{e}} + \dots, \quad (2)$$

where a dependency on the degeneracy q (as in a q -states Potts model) enters the first correction along with the inverse latent heat. Similarly, the inverse temperature $\beta^{B^{\min}}(L)$ where one finds



the minimum of Binder's energy parameter $B(\beta, L) = 1 - \langle E^4 \rangle / 3 \langle E^2 \rangle^2$ is predicted [10, 12],

$$\beta^{B^{\min}}(L) = \beta^\infty - \frac{\ln(q\hat{e}_o^2/\hat{e}_d^2)}{L^3\Delta\hat{e}} + \dots, \quad (3)$$

and apparently yields a $1/L^3$ correction to scaling too.

When a macroscopic degeneracy is present, we find that the scaling laws for periodic boundaries have to be adjusted, effectively enlarging the leading corrections [13]. A $3d$ plaquette (4-spin) interaction Ising model on a cubic lattice, where the Ising spins $\sigma_i = \pm 1$ live on the vertices of the lattice,

$$\mathcal{H} = -\frac{1}{2} \sum_{[i,j,k,l]} \sigma_i \sigma_j \sigma_k \sigma_l, \quad (4)$$

is a suitable candidate for investigating such behaviour, since its ground-state degeneracy of $q = 2^{3L}$ on an L^3 lattice is unbroken throughout the low-temperature phase [14]. The plaquette Hamiltonian is a member of a family of gonihedric Ising models which were originally formulated as a lattice discretization of a particular string-theory action [15]. It has attracted attention in its own right because it has a strong first-order transition [16] and displays evidence of glass-like behaviour at low temperatures [15, 17], in spite of the absence of quenched disorder.

If we take $q = 2^{3L}$ in Eqs. (2) and (3), as is the case for the plaquette Hamiltonian, we find

$$\beta^{C_V^{\max}}(L) = \beta^\infty - \frac{\ln(2^{3L})}{L^3\Delta\hat{e}} + \mathcal{O}\left(\frac{[\ln(2^{3L})]^2}{L^6}\right) = \beta^\infty - \frac{3\ln 2}{L^2\Delta\hat{e}} + \mathcal{O}(L^{-4}) \quad (5)$$

and

$$\beta^{B^{\min}}(L) = \beta^\infty - \frac{\ln(2^{3L}\hat{e}_o^2/\hat{e}_d^2)}{L^3\Delta\hat{e}} + \mathcal{O}\left(\frac{[\ln(2^{3L}\hat{e}_o^2/\hat{e}_d^2)]^2}{L^6}\right) = \beta^\infty - \frac{3\ln 2}{L^2\Delta\hat{e}} - \frac{\ln(\hat{e}_o^2/\hat{e}_d^2)}{L^3\Delta\hat{e}} + \mathcal{O}(L^{-4}) \quad (6)$$

so the leading contribution to the finite-size corrections is now $\propto 1/L^2$.

The modified scaling [13] has been extensively investigated by multicanonical simulations and found to be consistent, even with higher-order corrections for the inverse temperatures [18] and the maximum value of the specific heat [19]. The multicanonical Monte Carlo algorithm [20, 21] allows the system to quickly flip between the ordered and disordered phases, because the probability of unlikely states that hinder such fast transit is increased artificially. A weight function $W(\mathcal{H})$ that replaces the canonical Boltzmann weight $\exp(-\beta\mathcal{H})$ is improved recursively [22] so that we eventually get a flat multicanonical energy probability density. The weights are then fixed and the actual measurements are taken. The simulation converges towards the auxiliary multicanonical distribution as a fixed point and when the system is in equilibrium we can use the inverse of the weights to relate the measurements to their canonical Boltzmann weights. In this way, we achieve a double benefit from the algorithm. Firstly, the system is able to traverse highly improbable states to give a rapid oscillation between the ordered and disordered phases. Secondly, it is now possible to apply reweighting techniques over a much broader range of temperatures, since these need sufficient statistics in each bin of the histogram, which is naturally obtained from a flat histogram method.

For several lattice sizes L , we have simulated the model (4) with both fixed (all outer spins are set to +1) and periodic boundary conditions in Ref. [18] and measured observables such as the specific heat and Binder's energy parameter. Reweighting techniques allow the evaluation of those quantities as a function of temperature, and enable us to determine the positions of their peaks, $\beta^{C_V^{\max}}(L)$ and $\beta^{B^{\min}}(L)$ numerically with high precision. Along with the peak locations, we also calculated additional estimators $\beta^{\text{eqw}}(L)$ and $\beta^{\text{eqh}}(L)$ that relate to the double-peaked

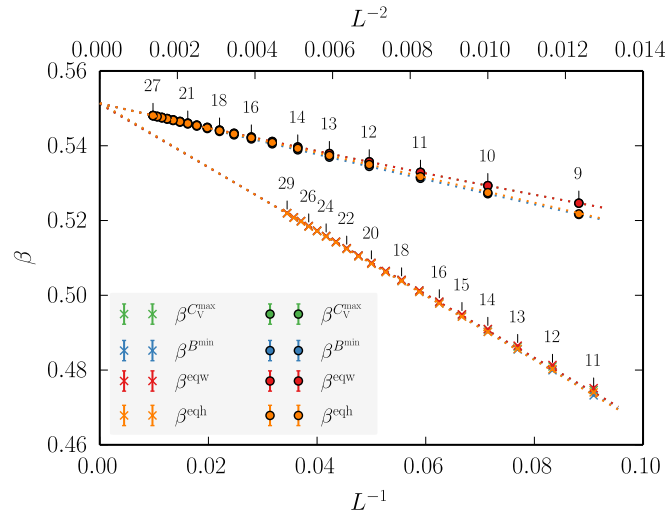


Figure 1. Finite-size scaling for periodic (upper abscissa) and fixed boundary conditions (lower abscissa) for the four inverse temperatures of the extremal values of the specific heat C_V^{\max} , Binder's energy parameter B^{\min} , or the difference of the peak weights or heights of the double-peaked energy probability density, D^{eqw} and D^{eqh} for various lattice sizes. Dotted lines are the extrapolations from the best fits, and small numbers give the linear lattice sizes for convenience.

canonical energy probability distribution $p(E, \beta)$. The energy of the minimum between the two peaks, E_{\min} , is determined to distinguish between the different phases and then used to minimize the difference of the peak *weights* or *heights*, respectively, namely

$$D^{\text{eqw}}(\beta) = \left(\sum_{E < E_{\min}} p(E, \beta) - \sum_{E \geq E_{\min}} p(E, \beta) \right)^2 \quad \text{and} \quad D^{\text{eqh}}(\beta) = \left(\max_{E < E_{\min}} \{p(E, \beta)\} - \max_{E \geq E_{\min}} \{p(E, \beta)\} \right)^2. \quad (7)$$

The data and fits in Fig. 1 for the estimates of the inverse transition temperature using Eqs. (5), (6) clearly display the non-standard scaling laws with $1/L^2$ corrections for periodic boundary conditions. The extrapolated values for the inverse temperature of the infinite system ($\beta^\infty = 0.551\,332(8)$) are visually and numerically in very good agreement with the somewhat less accurate values from the system with fixed boundaries ($\beta^\infty = 0.551\,38(5)$), where fits on the latter are conducted with a leading $1/L$ correction accounting for surface effects. The temperatures minimizing $D^{\text{eqw}}(\beta)$ and $D^{\text{eqh}}(\beta)$ in Eq. (7) also agree with the transmuted scaling behaviour for periodic boundaries and with $1/L$ scaling for fixed boundaries [18].

Apart from the transition temperature, another characteristic quantity that determines the dynamics at a first-order phase transition is the latent heat. The straightforward approach of measuring this in multicanonical simulations is to calculate the energies per site of the individual phases,

$$e_o(L) = \sum_{E < E_{\min}} e p(E, \beta^{\text{eqw}}) / \sum_{E < E_{\min}} p(E, \beta^{\text{eqw}}), \quad e_d(L) = \sum_{E \geq E_{\min}} e p(E, \beta^{\text{eqw}}) / \sum_{E \geq E_{\min}} p(E, \beta^{\text{eqw}}), \quad (8)$$

take their difference $\Delta e(L) = e_d(L) - e_o(L)$ and then extrapolate to the thermodynamic limit $L \rightarrow \infty$. This yields for periodic boundary conditions (bc) and lattice sizes up to $L = 27$ [18]

$$\Delta \hat{e} = 0.851\,48(5) \quad \text{periodic bc from (8)}, \quad (9)$$

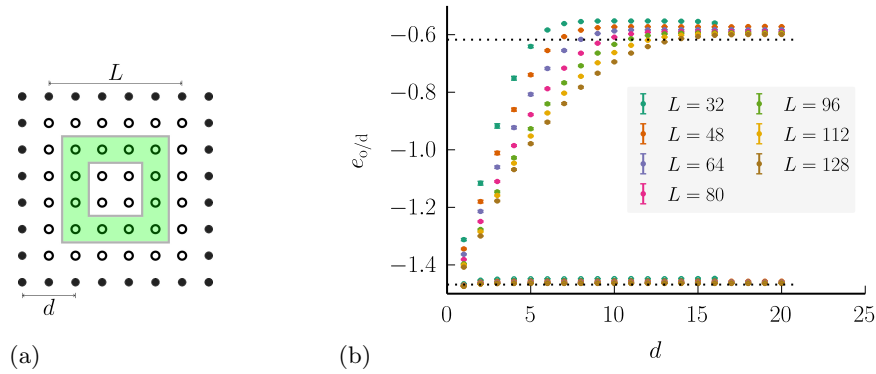


Figure 2. (a) Illustration of the setup of the simulations in a two-dimensional analogue. A cube of edge length L of free spins (represented by open circles) is surrounded by fixed spins with value +1 each (filled circles) and measurements are taken within a layer of width 1 at a distance d to the boundary (shaded area). (b) Energies of the disordered phase (upper data points) and ordered phase (lower data points) for different lattice sizes L . The dotted lines are the energies of the infinite system obtained from the multicanonical simulations. Both the ordered and disordered energies of the layers are overshooting the infinite lattice energies. Towards the boundary, the disordered phase becomes heavily perturbed by the fixed spins of the boundary.

and can be compared to Eqs. (5), (6), where we read off that the first correction of the non-standard finite-size scaling law only depends on the latent heat. The latent heat obtained by the fitting parameters was found to be consistent [18], although tending slightly to higher values.

For the fixed boundary conditions, measuring similarly the energy from an extrapolation of lattice sizes up to $L = 29$ [18] gives a much smaller latent heat of

$$\Delta\hat{e} = 0.694(4) \quad \text{fixed bc from (8) ,} \quad (10)$$

which is puzzling since this is not in accordance with the expectation that contributions from the boundary vanish in the thermodynamic limit.

To clarify this curious feature, we prepared short (canonical) Metropolis simulations for systems up to much larger linear sizes $L \in \{32, 48, 64, 80, 96, 112, 128\}$ and fixed boundaries. The systems were prepared in the disordered or ordered phases at a fixed temperature given by

$$\beta^{\text{eqw}}(L) = 0.551\,19(12) - 0.8486(25)/L , \quad (11)$$

where we used the best fit of Ref. [18] obtained for fixed boundaries. In a first approximation, the system then has an equal probability to be in the disordered or ordered phases and, taking advantage of the huge free-energy barrier between them [18], we made sure that *no* “tunneling” between the phases occurs during the canonical simulations. We perform a number of $2^{16} = 65\,536$ sweeps and discard the first half of the time series, where thermalization effects may hamper the measurements. Effectively, we have a number of $2^{15} = 32\,768$ (correlated) measurements of the energy in each of the different phases. The statistical errors are then computed by Jackknife analysis using 16 blocks.

The influence of the fixed boundary is investigated by taking measurements in layers of unit-width at several distances d to the fixed boundary around a bigger cube of linear system size L as illustrated in Fig. 2(a). To have the energy of the layers normalized without trivial bias, the local energy at a given spin (the sum over all plaquettes touching that spin) is divided by

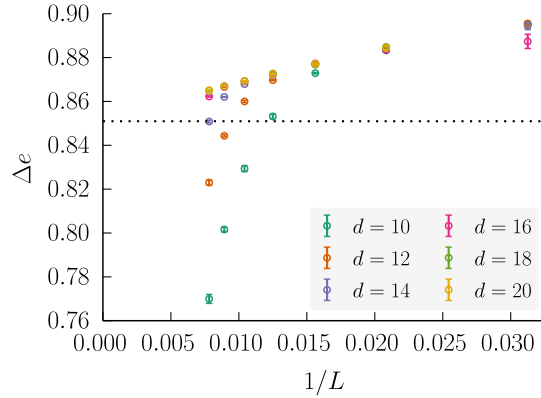


Figure 3. The latent heat over inverse lattice length L in layers at a distance d for the measurements from Fig. 2(b) at several d . The expected latent heat as $1/L \rightarrow 0$ obtained from multicanonical simulations with periodic boundary conditions is denoted by the dotted line.

the 12 possibly activated plaquettes. This is averaged over all spins in the layer and multiplied by a factor of 3 to keep the same energetic scale¹ as in Ref. [18]. The energies of the ordered and disordered phases $e_{o/d}$ obtained in this way as a function of the distance d are collected in Fig. 2(b). With decreasing distance, the layers get increasingly ordered, which is reflected by both curves bending towards the ground-state energy $e = -1.5$. We find that far from the boundary the energies are overshooting the infinite volume limits. This is in accordance with the Taylor series expansion of the energies around $\beta = \beta^\infty$,

$$e_{o/d}(\beta) = \hat{e}_{o/d} + \left. \frac{\partial e_{o/d}}{\partial \beta} \right|_{\beta=\beta^\infty} (\beta - \beta^\infty) + \mathcal{O}((\beta - \beta^\infty)^2), \quad (12)$$

which leads to

$$e_{o/d}(\beta^{\text{eqw}}) = \hat{e}_{o/d} - \hat{C}_{o/d} \left(\frac{1}{\beta^\infty} \right)^2 (\beta^{\text{eqw}} - \beta^\infty) + \mathcal{O}((\beta^{\text{eqw}} - \beta^\infty)^2). \quad (13)$$

Here, the specific heats $\hat{C}_{o/d} = -(\beta^2 \partial e_{o/d} / \partial \beta)|_{\beta=\beta^\infty}$ of the pure phases enter and the (empirical) first correction $\beta^{\text{eqw}} - \beta^\infty < 0$ from Eq. (11) gives

$$e_{o/d}(\beta^{\text{eqw}}) = \hat{e}_{o/d} + 0.8486(25) \hat{C}_{o/d} \left(\frac{1}{\beta^\infty} \right)^2 / L + \dots \quad (14)$$

Therefore the first correction to the energies is a positive value and we would expect the energies of the ordered and disordered phase to be larger than those for infinite volume, as measured.

The spatial range of the perturbation of the disordered phase by the fixed boundary spins is somewhat unexpected. For the simulated lattice sizes, the disordered energy is retrieved first at a distance of at least $d = 14$. At this distance, already 52% of the total number of spins reside in the boundary of a $L = 128$ cube, which means that one must neglect more than

¹ For periodic boundaries, dividing by the number of spins L^3 instead of the number of plaquettes $3L^3$ leaves an additional factor of 3 in the energy scale. For fixed boundaries the number of plaquettes is $3L(L+1)^2$ when L is the linear lattice length of free spins and only those plaquettes that are composed of at most three *fixed* spins are added to the system's energy.

half of the interactions in the system to find an unperturbed disordered energy. This implies that the extrapolation of the latent heat in [18] is clearly obscured, where only lattices up to linear size $L = 29$ were accessible. The latent heat contained in layers at several distances from the boundary as a function of the inverse linear lattice size is shown Fig. 3, to qualitatively understand the scaling of the energies within the layers. With increasing distance d , fits would yield increasingly higher values as $L \rightarrow \infty$, at least asymptotically bigger than that of 0.694(4) in Eq. (10). To further elaborate on this, a fit on the asymptotics of the latent heat contained in the layer at $d = 20$ yields $\Delta e(L) = 0.8530(3) + 1.56(3)/L$ with $\chi^2_{\text{dof}} = 1.15$, which is much closer to 0.85148(5) from the simulations with periodic boundary conditions.

Any model with an exponentially degenerate low-temperature phase will display the modified scaling at a first-order phase transition described for the 3d gonihedric model here. Apart from higher-dimensional variants of the gonihedric model or its dual [18], there are numerous other fields where the scenario could be realized. Examples range from ANNNI models [23] to topological “orbital” models in the context of quantum computing [24] such as the 3d classical compass or t_{2g} orbital model where a highly degenerate ground state is well known and signatures of a first-order transition into the disordered phase have recently been found numerically [25].

Acknowledgements

This work was supported by the Deutsche Forschungsgemeinschaft (DFG) through the Collaborative Research Centre SFB/TRR 102 (project B04) and by the Deutsch-Französische Hochschule (DFH-UFA) under Grant No. CDFA-02-07.

- [1] Janke W 2003 *First-order phase transitions in Computer Simulations of Surfaces and Interfaces* (NATO Science Series, II. Math., Phys. and Chem. 114) eds B Dünweg, D P Landau and A I Milchev (Dordrecht: Kluwer) pp 111–135, and references therein
- [2] Imry Y 1980 *Phys. Rev. B* **21** 2042
- [3] Binder K 1981 *Z. Phys. B* **43** 119
- [4] Fisher M E and Berker A N 1982 *Phys. Rev. B* **26** 2507
- [5] Privman V and Fisher M E 1983 *J. Stat. Phys.* **33** 385
- [6] Binder K and Landau D P 1984 *Phys. Rev. B* **30** 1477
- [7] Challa M S S, Landau D P and Binder K 1986 *Phys. Rev. B* **34** 1841
- [8] Peczak P and Landau D P 1989 *Phys. Rev. B* **39** 11932
- [9] Privman V and Rudnik J 1990 *J. Stat. Phys.* **60** 551
- [10] Janke W 1993 *Phys. Rev. B* **47** 14757
- [11] Borgs C and Kotecký R 1990 *J. Stat. Phys.* **61** 79; 1992 *Phys. Rev. Lett.* **68** 1734
- [12] Borgs C and Janke W 1992 *Phys. Rev. Lett.* **68** 1738
- [13] Mueller M, Janke W and Johnston D A 2014 *Phys. Rev. Lett.* **112** 200601
- [14] Pietig R and Wegner F 1996 *Nucl. Phys. B* **466** 513; 1998 *Nucl. Phys. B* **525** 549
- [15] Johnston D A, Lipowski A and Malmgren R P K C 2008 *The gonihedric Ising model and glassiness in Rugged Free-Energy Landscapes – An Introduction* (Springer Lecture Notes in Physics vol 736) ed W Janke (Berlin/Heidelberg: Springer) pp 173–199, and references therein
- [16] Espriu D, Baig M, Johnston D A and Malmgren R P K C 1997 *J. Phys. A: Math. Gen.* **30** 405
- [17] Lipowski A 1997 *J. Phys. A: Math. Gen.* **30** 7365
- [18] Mueller M, Johnston D A and Janke W 2014 *Nucl. Phys. B* **888** 214
- [19] Mueller M, Janke W and Johnston D A 2014 *Physics Procedia* **57** 68
- [20] Berg B A and Neuhaus T 1991 *Phys. Lett. B* **267** 249; 1992 *Phys. Rev. Lett.* **68** 9
- [21] Janke W 1992 *Int. J. Mod. Phys. C* **03** 1137; 1998 *Physica A* **254** 164
- [22] Janke W 2003 *Histograms and all that in Computer Simulations of Surfaces and Interfaces* (NATO Science Series, II. Math., Phys. and Chem. 114) eds B Dünweg, D P Landau and A I Milchev (Dordrecht: Kluwer) pp 137–157, and references therein
- [23] Selke W 1988 *Phys. Rep.* **170** 213
- [24] Nussinov Z and van den Brink J 2013 Compass and Kitaev models – Theory and physical motivations *e-print arXiv:1303.5922*
- [25] Gerlach M H and Janke W 2015 *Phys. Rev. B* **91** 045119